



Comparison of ^{18}F -GE-180 and dynamic ^{18}F -FET PET in high grade glioma: a double-tracer pilot study

Marcus Unterrainer^{1,2} · D. F. Fleischmann^{2,3} · C. Diekmann¹ · L. Vomacka¹ · S. Lindner¹ · F. Vettermann¹ · M. Brendel¹ · V. Wenter¹ · B. Ertl-Wagner⁴ · J. Herms⁵ · C. Wetzel⁶ · R. Rupprecht⁶ · J. C. Tonn^{2,7} · C. Belka^{2,3} · P. Bartenstein^{1,2} · M. Niyazi^{2,3} · Nathalie L. Albert^{1,2}

Received: 22 May 2018 / Accepted: 11 September 2018 / Published online: 22 September 2018
© Springer-Verlag GmbH Germany, part of Springer Nature 2018

Abstract

Background PET represents a valuable tool for glioma imaging. In addition to amino acid tracers such as ^{18}F -FET, PET targeting the 18-kDa mitochondrial translocator-protein (TSPO) is of high interest for high-grade glioma (HGG) imaging due to its upregulation in HGG cells. ^{18}F -GE-180, a novel TSPO ligand, has shown a high target-to-background contrast in HGG. Therefore, we intra-individually compared its uptake characteristics to dynamic ^{18}F -FET PET and contrast-enhanced MRI in patients with HGG.

Methods Twenty HGG patients (nine *IDH*-wildtype, 11 *IDH*-mutant) at initial diagnosis ($n = 8$) or recurrence ($n = 12$) were consecutively included and underwent ^{18}F -GE-180 PET, dynamic ^{18}F -FET PET, and MRI. The maximal tumour-to-background ratios (TBR_{max}) and biological tumour volumes (BTV) were evaluated in ^{18}F -GE-180 and ^{18}F -FET PET. Dynamic ^{18}F -FET PET analysis included the evaluation of minimal time-to-peak (TTP_{min}). In MRI, the volume of contrast-enhancement was delineated (VOL_{CE}). Volumes were spatially correlated using the Sørensen–Dice coefficient.

Results The median TBR_{max} tended to be higher in ^{18}F -GE-180 PET compared to ^{18}F -FET PET [4.58 (2.33–8.95) vs 3.89 (1.56–7.15); $p = 0.062$] in the overall group. In subgroup analyses, *IDH*-wildtype gliomas showed a significantly higher median TBR_{max} in ^{18}F -GE-180 PET compared to ^{18}F -FET PET [5.45 (2.56–8.95) vs 4.06 (1.56–4.48); $p = 0.008$]; by contrast, no significant difference was observed in *IDH*-mutant gliomas [3.97 (2.33–6.81) vs 3.79 (2.01–7.15) $p = 1.000$]. Only 5/20 cases showed higher TBR_{max} in ^{18}F -FET PET compared to ^{18}F -GE-180 PET, all of them being *IDH*-mutant gliomas. No parameter in ^{18}F -GE-180 PET correlated with TTP_{min} ($p > 0.05$ each). There was a tendency towards higher median $\text{BTV}_{\text{GE-180}}$ [32.1 (0.4–236.0) ml] compared to BTV_{FET} [19.3 (0.7–150.2) ml; $p = 0.062$] with a moderate spatial overlap [median Sørensen–Dice coefficient 0.55 (0.07–0.85)]. In MRI, median VOL_{CE} [9.7 (0.1–72.5) ml] was significantly smaller than both BTV_{FET} and $\text{BTV}_{\text{GE180}}$ ($p < 0.001$ each), leading to a poor spatial correlation with $\text{BTV}_{\text{GE-180}}$ [0.29 (0.01–0.48)] and BTV_{FET} [0.38 (0.01–0.68)].

Conclusion PET with ^{18}F -GE-180 and ^{18}F -FET provides differing imaging information in HGG dependent on the *IDH*-mutational status, with diverging spatial overlap and vast exceedance of contrast-enhancement in MRI. Combined PET imaging might reveal new insights regarding non-invasive characterization of tumour heterogeneity and might influence patients' management.

Electronic supplementary material The online version of this article (<https://doi.org/10.1007/s00259-018-4166-1>) contains supplementary material, which is available to authorized users.

✉ Nathalie L. Albert
nathalie.albert@med.uni-muenchen.de

Marcus Unterrainer
marcus.unterrainer@med.uni-muenchen.de

¹ Department of Nuclear Medicine, University Hospital, LMU Munich, Marchioninstr. 15, 81377 Munich, Germany

² German Cancer Consortium (DKTK), Partner Site Munich; and German Cancer Research Center (DKFZ), Heidelberg, Germany

³ Department of Radiation Oncology, University Hospital, LMU Munich, Marchioninstr. 15, 81377 Munich, Germany

⁴ Institute of Clinical Radiology, University Hospital, LMU Munich, Marchioninstr. 15, 81377 Munich, Germany

⁵ Department of Neuropathology, University Hospital, LMU Munich, Marchioninstr. 15, 81377 Munich, Germany

⁶ Department of Psychiatry and Psychotherapy, University of Regensburg, Regensburg, Germany

⁷ Department of Neurosurgery, University Hospital, LMU Munich, Marchioninstr. 15, 81377 Munich, Germany

Keywords ^{18}F -GE-180 · TSPO · ^{18}F -FET · Amino acid · MRI · High-grade glioma

Introduction

The diagnostic gold standard for high-grade glioma (HGG) imaging is represented by magnetic resonance imaging (MRI), with contrast-enhancement indicating blood–brain-barrier (BBB) breakdown in MRI [1]. A major challenge during planning of local treatments such as radiotherapy or surgical resection is the delineation of the tumour extent beyond contrast enhancement (CE) in MRI, as the ‘real tumour extent’ knowingly exceeds the areas of CE in MRI [2, 3]. Therefore, positron emission tomography (PET) using a variety of radiotracers, in particular radiolabeled amino acids such as *O*-(2- ^{18}F fluoroethyl)-L-tyrosine (^{18}F -FET), is increasingly used for glioma imaging in clinical routine as a valuable complementary tool to conventional MRI images [4, 5]. On a molecular level, an increased expression of system-L-amino acid transporters (LAT) is responsible for tumoral ^{18}F -FET-uptake [6]. Although ^{18}F -FET PET is considered a reliable modality for delineating tumour tissue, parts of a glioma or an entire glioma can be ^{18}F -FET-negative, which is observed in one third of low-grade gliomas and can even occur in high-grade gliomas [7].

In addition to the uptake of amino acids, the 18-kDa mitochondrial translocator protein (TSPO) represents a promising target for PET imaging. Being located at the outer mitochondrial membrane, TSPO is expressed by activated microglia and macrophages in neuroinflammatory processes. In addition, TSPO is also expressed in HGG cells themselves, enabling PET-ligands to visualize the TSPO in high-grade gliomas non-invasively. Although the role of TSPO in HGG is not fully understood, it has been reported to be attributable to aggressive tumour features [8]. By contrast, there is only a low expression in cells of low-grade gliomas (LGG) [9]. Within recent years, first preclinical studies have been published testing TSPO PET tracers for in-vivo imaging of gliomas [10–13] and have indicated promising results, whereas only a limited number of TSPO PET studies have been performed in humans so far [9, 14–16]. In these studies, TSPO ligands of the previous generation such as ^{11}C -(*R*)PK11195 were used, but harbored major disadvantages such as a low binding affinity or short half-life of [^{11}C]. Recently, ^{18}F -GE-180, a novel tricyclic indole TSPO ligand of the latest generation with high binding affinity [17–19], has shown superior imaging properties compared to other previous tracers [18, 20]. Moreover, TSPO imaging in healthy humans [21, 22] and patients suffering from relapsing-remitting multiple sclerosis [23, 24] showed high feasibility. In gliomas, we showed that ^{18}F -GE-180 PET in patients with glioblastoma provides a high tumour-to-background contrast and a distinct exceedance of contrast-enhancing tumour parts in MRI [25].

As a recent study with limited sample size indicated a considerable discrepancy of tumoral TSPO expression, as assessed with ^{123}I -CLINDE SPECT, and amino acid uptake using the clinically established amino acid tracer ^{18}F -FET in a set of three glioblastoma patients [26], we hypothesized that TSPO expression, amino acid uptake, and CE do visualize partially different tumour parts, possibly depending on the tumour grade and molecular genetic features. Therefore, we intra-individually compared and spatially correlated the tumoral TSPO expression, dynamic amino acid uptake, and contrast enhancement in patients with newly diagnosed and recurrent HGG using the novel PET-ligand ^{18}F -GE-180, dynamic ^{18}F -FET PET, and contrast-enhanced MRI, and correlated these findings with the individual tumour grading and molecular genetic profile.

Materials and methods

Patients

Patients with HGG at initial diagnosis or recurrence prior to any further therapy were consecutively included in this pilot study. Newly diagnosed brain tumours were verified by histology; HGG recurrence was evaluated by histology or, in cases of missing clinical indication for stereotactic biopsy or resection, according to Response Assessment in Neuro-Oncology (RANO) working group criteria for HGG [1] without any suspicion of treatment-related changes. Prior to further therapies, the included patients underwent ^{18}F -GE-180 PET and dynamic ^{18}F -FET PET. Additionally, all individuals underwent genotyping for polymorphism of the TSPO gene. This study was approved by the local ethics committee, and all patients gave written informed consent (IRB no. 17–769).

Histological confirmation, tumour grading, and molecular genetic analysis

Stereotactic biopsy procedures and microsurgical resections were performed at the Department of Neurosurgery, LMU Munich, Germany. As part of the clinical routine, histopathological and molecular genetic evaluations (*IDH*-mutation, 1p/19q-codeletion) were performed at the Institute of Neuropathology, LMU Munich, Germany, and were classified according to the updated WHO 2016 classification of brain tumours [27]. For further specifications regarding the histopathological workup, see also [28, 29].

DNA extraction and polymorphism genotyping

Due to the known dependency on a genetic polymorphism of the TSPO gene of binding properties of the TSPO ligands of the previous generation [30–32], all patients underwent genotyping and were consequently evaluated as low-, medium- or high-affinity binders (LAB, MAB, and HAB respectively). For this purpose, whole blood samples were sent to the Department of Psychiatry and Psychotherapy, University of Regensburg, Germany, for polymorphism genotyping. For further specifications, see also [23, 24].

PET acquisition

All patients were scanned at the Department of Nuclear Medicine, LMU Munich, with a Biograph 64 PET/CT scanner (Siemens, Erlangen, Germany). A low-dose CT scan preceded the PET acquisition and served for attenuation correction. Images of both tracers were reconstructed using OSEM3D algorithm (eight iterations, four subsets, 4 mm Gauss) with a matrix size of $336 \times 336 \times 109$, a voxel size of $1.018 \times 1.018 \times 2.027 \text{ mm}^3$, and a slice thickness of 2.027 mm. For each scan, standard corrections for attenuation, scatter, decay, and random counts were applied. Automated production of ^{18}F -GE-180 was performed as published previously [23, 33]. After injection of $178 \pm 12 \text{ MBq } ^{18}\text{F}$ -GE-180 as intravenous bolus, data were acquired 60–80 min p.i.; the respective summation images were used for image analysis [25]. After injection of $174 \pm 23 \text{ MBq } ^{18}\text{F}$ -FET as intravenous bolus, data were acquired 0–40 min p.i. Summation images 20–40 min p.i. were used for static and 0–40 min data were used for dynamic analysis.

Magnetic resonance imaging

As part of the clinical routine, patients underwent MRI scans with a slice thickness of 1 mm. In all patients, axial T2-weighted sequences as well as T1-weighted sequences before and after intravenous administration of 0.1 mmol/kg gadobenate dimeglumine contrast agent (Gd-BOPTA, MultiHance®; BraccoImaging, Milan, Italy) were acquired. Volumes of contrast-enhancement (CE) excluding necrosis (VOL_{CE}) were manually delineated in the fused T1 images using the PMOD Neuro tool (v3.5, PMOD Technologies, Zurich, Switzerland) after consensus reading.

Image evaluation

^{18}F -FET PET The mean background activity (BG) was assessed in the healthy contralateral hemisphere as previously published [34]. The biological tumour volume (BTV) was estimated by a semiautomatic threshold-based delineation of a volume of interest (VOI), using a standardized uptake value (SUV)

threshold of $1.8 \times \text{BG}$ [3], resulting in BTV_{FET} . For the assessment of the maximal tumour-to-background ratio (TBR_{max}), the maximal SUV was divided by the BG. As described previously [35], dynamic PET data were evaluated using the software PET Display Dynamic implemented in the Hermes workstation (Hermes Medical Solutions, Stockholm, Sweden); the time–activity curves were evaluated on a slice-by-slice basis, the time to peak (TTP) was assessed in each slice within the tumour; the shortest TTP in at least two consecutive slices was defined as minimal TTP (TTP_{min}), see also [36].

^{18}F -GE-180 PET BG and TBR_{max} were assessed analogously to ^{18}F -FET PET. The TSPO-positive PET volumes were semi-automatically delineated using the commonly applied threshold $\text{SUV}_{\text{BG}} \times 1.8$ ($\text{BTV}_{\text{GE-180}}$), as no histologically verified threshold exists for TSPO PET so far [25].

Moreover, the relative TBR_{max} as defined as the individual ratio of both tracers was assessed, i.e., relative $\text{TBR}_{\text{max}} = \text{TBR}_{\text{max}} ^{18}\text{F}$ -GE180 / ^{18}F -FET. Image analysis was performed using PMOD Neuro tool (v3.5, PMOD Technologies, Zurich, Switzerland). ^{18}F -GE-180 and ^{18}F -FET PET images were automatically coregistered with contrast-enhanced, T1-weighted MRI images, and visually screened for correct positioning. Volumes of CE, ^{18}F -GE-180 PET, and ^{18}F -FET PET were then spatially correlated using the Sørensen–Dice coefficient, as defined as two times the ratio between the respective intersection volume and the sum of both volumes, i.e., $2 \times | \text{Volume}_1 \cap \text{Volume}_2 | / (| \text{Volume}_1 | + | \text{Volume}_2 |)$ [37, 38].

Statistical analysis

Statistical analysis was performed with IBM® SPSS® Statistics, Version 24. Descriptive statistics were used for patients' characteristics and PET parameters. Normal distribution was assessed by Shapiro–Wilk test. Descriptive statistics are displayed as median (range). Comparing continuous non-parametric parameters, Mann–Whitney U test was used for independent variables and Wilcoxon signed-rank test for dependent paired variables. Kruskal–Wallis test was used for comparisons of non-parametric and unpaired parameters within more than two groups. Non-parametric continuous variables were correlated using Spearman's rank correlation coefficient. Statistical significance was defined as two-tailed p -values < 0.05 . In cases of low p -values not reaching the level of significance (i.e., p -values 0.05–0.065), the term “tended” was used.

Results

Patients

Twenty HGG patients [11 female, nine male; median age 49.8 years (range, 29.1–69.8 years)] were consecutively

included in 2017. Of these, 8/20 patients (40.0%) presented with newly-diagnosed and 12/20 (60%) with recurrent glioma. *IDH*-mutation was present in 11/20 of the included gliomas (55%; 8/11 WHO grade III, 3/11 WHO grade IV); 9/20 cases were *IDH*-wildtype gliomas (45%; 2/9 WHO grade III, 7/9 WHO grade IV). Histological validation was performed in all newly diagnosed (7/8 stereotactic biopsy, 1/8 resection after imaging) and in 8/12 recurrent HGG (7/8 stereotactic biopsy, 1/8 resection after imaging). Four further recurrent gliomas with progressive disease according to RANO criteria [1] without any suspicion of treatment-related changes were included; these cases had undergone histological and molecular genetic work-up in the previous disease course (four WHO grade III, *IDH*-mutant). Genotyping for the *TSPO*-polymorphism revealed 12/20 (60%) patients with HAB, 5/20 (25%) with MAB, and 3/20 (15%) with LAB status. The median interval between ^{18}F -GE-180 and ^{18}F -FET PET was 3 days (range, 1–15 days), between ^{18}F -GE-180 PET and MRI 15 days (range, 0–30 days) and between ^{18}F -FET PET and MRI 14 days (range, 0–30 days). See Tables 1 and 2.

^{18}F -GE-180 PET parameters

Overall, the median TBR_{max} was 4.58 (range, 2.33–8.95) and the median $\text{BTV}_{\text{GE-180}}$ 32.1 ml (range, 0.4–236.0 ml). In

subgroup analyses, *IDH*-wildtype gliomas showed a higher TBR_{max} (median 5.44 (range, 2.56–8.95) vs 3.97 (range, 2.33–6.81) compared to *IDH*-mutant gliomas without reaching the level of significance ($p = 0.080$). Moreover, there were no significantly different ^{18}F -GE-180 PET TBR_{max} or $\text{BTV}_{\text{GE-180}}$ values comparing newly diagnosed and recurrent glioma ($p > 0.05$ each). See Tables 2 and 3.

^{18}F -FET PET parameters

In the overall group, the median TBR_{max} was 3.83 (range, 1.56–7.15) and the median BTV_{FET} was 19.3 ml (range, 0.7–150.2 ml). In one patient, the tumoral uptake did not exceed the background activity (i.e., $< 1.8 \times \text{BG}$); thus, no BTV_{FET} was delineated (anaplastic astrocytoma, *IDH*-wildtype). The dynamic evaluation revealed a median TTP_{min} of 17.5 min (4.0–35.0 min) in the overall group; in one patient, TTP_{min} could not be evaluated due to technical reasons.

In contrast to ^{18}F -GE-180 PET, ^{18}F -FET PET analyses revealed no different median TBR_{max} in *IDH*-wildtype compared to *IDH*-mutant gliomas [4.06 (range, 1.56–4.49) vs 3.79 (range, 2.01–7.14); $p = 0.776$]. Also, there were no significantly different ^{18}F -FET PET parameters comparing

Table 1 Overview of patients' characteristics

Patient	Diagnosis	WHO grade	<i>IDH</i> -mutation	1p/19q-codeletion	MGMT-methylation	Stage	Evaluation
1	GBM	IV	No	No	No	Recurrence	Biopsy
2	GBM	IV	Yes	No	Yes	Recurrence	Biopsy
3	GBM	IV	Yes	No	Yes	Recurrence	Biopsy
4	AA	III	Yes	No	Yes	Initial diagnosis	Biopsy
5	AA	III	Yes	No	Yes	Recurrence	RANO
6	AA	III	Yes	No	Yes	Recurrence	RANO
7	AOD	III	Yes	Yes	Yes	Recurrence	RANO
8	GBM	IV	No	No	No	Initial diagnosis	Biopsy
9	AOD	III	Yes	Yes	Yes	Initial diagnosis	Biopsy
10	AOD	III	Yes	Yes	Yes	Recurrence	Biopsy
11	GBM	IV	No	No	Yes	Initial diagnosis	Biopsy
12	AA	III	Yes	No	Yes	Recurrence	RANO
13	GBM	IV	Yes	No	Yes	Recurrence	Resection
14	AOD	III	Yes	Yes	Yes	Recurrence	Biopsy
15	AA	III	No	No	No	Initial diagnosis	Biopsy
16	GBM	IV	No	No	Yes	Initial diagnosis	Resection
17	GBM	IV	No	No	No	Recurrence	Biopsy
18	GBM	IV	No	No	Yes	Recurrence	Biopsy
19	AA	III	No	No	No	Initial diagnosis	Biopsy
20	GBM	IV	No	No	No	Initial diagnosis	Biopsy

GBM = glioblastoma; AA = anaplastic astrocytoma; AOD = anaplastic oligodendroglioma; RANO = response assessment in neurooncology

newly diagnosed and recurrent glioma ($p > 0.05$ each). See Tables 2 and 3.

Comparison of uptake intensity in ^{18}F -GE-180 and ^{18}F -FET PET

Overall, the median TBR_{max} in ^{18}F -GE-180 PET tended to be higher compared to ^{18}F -FET PET [4.58 (range, 2.33–8.95) vs 3.83 (range, 1.56–7.15); $p = 0.062$], without reaching the level of significance. In the subgroup of *IDH*-wildtype gliomas, the median TBR_{max} was significantly higher in ^{18}F -GE-180 PET compared to ^{18}F -FET PET [5.44 (2.56–8.95) vs 4.06 (range, 1.56–4.49); $p = 0.008$]. In contrast, in the subgroup of *IDH*-mutant gliomas, the median TBR_{max} was statistically indifferent comparing ^{18}F -GE-180 and ^{18}F -FET PET ($p > 0.05$); see also Table 3.

In the majority of patients (15/20 cases), the uptake intensity was higher in ^{18}F -GE-180 PET compared to ^{18}F -FET PET; all the remaining five cases with higher uptake in ^{18}F -FET PET were *IDH*-mutant gliomas. None of the parameters in ^{18}F -GE-180 PET correlated with TTP_{min} ($p > 0.05$ each), as derived in dynamic ^{18}F -FET PET.

Comparable results could be obtained in subgroup analyses with regard to WHO grades with higher uptake of ^{18}F -GE-180 compared to ^{18}F -FET in the more aggressive WHO grade IV gliomas and no significant differences in the subgroup of WHO grade III gliomas; see Tables 2 and 3.

Overall, a median relative TBR_{max} (i.e., TBR_{max} ratio ^{18}F -GE-180 / ^{18}F -FET) of 1.23 (range, 0.44–2.05) was observed, i.e., a 1.23-fold higher TBR_{max} could be observed in ^{18}F -GE-180 compared to ^{18}F -FET PET in median. In the subgroup analysis, *IDH*-wildtype gliomas showed a median relative TBR_{max} of 1.55 (range, 1.04–2.05), which was significantly higher than in *IDH*-mutant gliomas with a median relative TBR_{max} of 1.05 (range, 0.44–1.60; $p = 0.012$). This could not be shown in the subgroup analyses of WHO grades [WHO IV: median 1.46 (range, 0.95–2.05), WHO III: median 1.12 (0.44–2.05), $p = 0.218$].

For the comparison of plain SUV values, please see supplementary Tab. 1.

Spatial correlation of PET derived BTVs

Evaluating absolute volumes, median $\text{BTV}_{\text{GE-180}}$ [32.1 ml (range, 0.4–236.0 ml)] was higher than BTV_{FET} [19.3 ml

Table 2 Overview patients' PET specifications

Patient	MRI		^{18}F -GE-180 PET				^{18}F -FET PET			Sørensen–Dice coefficients		
	CE	VOL_{CE} [ml]	Binding status	SUV_{BG}	TBR_{max}	$\text{BTV}_{\text{GE-180}}$ [ml]	TBR_{max}	BTV_{FET} [ml]	TTP_{min} [min]	$\text{BTV}_{\text{GE-180}}$ vs BTV_{FET}	VOL_{CE} vs BTV_{FET}	VOL_{CE} vs $\text{BTV}_{\text{GE-180}}$
1	Yes	43.2	HAB	0.41	4.05	52.1	3.23	19.3	n.a.	0.67	0.46	0.38
2	Yes	50.5	MAB	0.36	4.58	135.9	2.96	65.3	17.5	0.31	0.37	0.18
3	Yes	1.5	MAB	0.36	6.81	31.6	7.15	26.2	7.5	0.74	0.07	0.09
4	No	–	HAB	0.37	2.38	0.4	2.01	0.7	17.5	0.11	–	–
5	Yes	9.5	HAB	0.39	3.97	99.0	3.79	45.6	17.5	0.67	0.15	0.23
6	Yes	22.1	LAB	0.47	4.47	71.2	3.69	19.0	17.5	0.65	0.54	0.45
7	Yes	2.1	HAB	0.4	2.33	2.0	5.29	12.7	7.5	0.09	0.09	0.06
8	Yes	2.2	HAB	0.32	6.38	13.0	4.10	7.1	4.0	0.85	0.31	0.28
9	Yes	0.4	HAB	0.35	2.77	0.8	3.87	16.0	35.0	0.04	0.03	0.32
10	Yes	6.7	HAB	0.46	2.74	3.1	3.74	7.3	25.0	0.18	0.27	0.26
11	Yes	9.9	LAB	0.37	8.95	59.0	4.37	31.5	25.0	0.66	0.34	0.31
12	Yes	39.6	MAB	0.54	3.43	27.0	5.64	117.9	7.5	0.26	0.12	0.05
13	Yes	15.7	MAB	0.47	4.57	52.4	3.15	20.0	25	0.67	0.36	0.43
14	Yes	12.2	MAB	0.36	6.81	32.7	4.25	13.4	4.0	0.69	0.66	0.53
15	No	–	HAB	0.34	2.56	1.0	1.56	–	17.5	–	–	–
16	Yes	72.5	HAB	0.40	6.55	236.0	4.47	150.2	12.5	0.83	0.54	0.44
17	Yes	2.6	HAB	0.49	4.78	15.6	4.06	8.8	12.5	0.54	0.23	0.31
18	Yes	14.7	LAB	0.45	6.27	121.1	3.34	25.3	25.0	0.41	0.50	0.22
19	Yes	0.0	HAB	0.39	5.44	3.8	2.65	2.5	7.5	0.28	0.01	0.01
20	Yes	0.5	HAB	0.43	4.67	156.8	4.49	101.2	7.5	0.59	0.57	0.34

HAB = high-affinity binder; MAB = medium-affinity binder; LAB = low-affinity binder; CE = contrast enhancement; n.a. = not available

Table 3 Distribution of TBR_{max} in ¹⁸F-GE180 and ¹⁸F-FET PET [median (range)]

	¹⁸ F-GE180 PET	¹⁸ F-FET PET	Significance
Total	4.58 (2.33–8.95)	3.83 (1.56–7.15)	<i>p</i> = 0.062
<i>IDH</i> -mutant	3.97 (2.33–6.81)	3.79 (2.01–7.15)	<i>p</i> = 1.000
<i>IDH</i> -wildtype	5.45 (2.56–8.95)	4.06 (1.56–4.48)	<i>p</i> = 0.008
Significance	<i>p</i> = 0.080	<i>p</i> = 0.766	
WHO grade III	3.10 (2.33–4.48)	3.65 (1.56–5.64)	<i>p</i> = 0.959
WHO grade IV	5.52 (4.05–8.95)	4.08 (2.96–7.15)	<i>p</i> = 0.009
Significance	<i>p</i> = 0.005	<i>p</i> = 0.481	

(range, 0.7–150.2 ml)], without reaching the level of significance (*p* = 0.062). In the intra-individual spatial comparison of tumour volumes, there was only a moderate spatial overlap of the BTVs (BTV_{GE-180} vs BTV_{FET}), with a median Sørensen–Dice coefficient of 0.55 (range, 0.07–0.85). In the subgroups, *IDH*-wildtype and *IDH*-mutant gliomas showed a comparable degree of spatial overlap of BTV_{GE-180} and BTV_{FET} (median Sørensen–Dice coefficient 0.53 [range, 0.07–0.76] vs 0.59 (range, 0.32–0.85), *p* = 0.206], whereas the spatial overlap was lower in the group of WHO grade III gliomas compared to WHO grade IV gliomas [0.33 (range, 0.07–0.63) vs 0.62 (range, 0.20–0.85); *p* = 0.065], without reaching the level of significance. For further specifications see Table 4.

Correlation of PET with contrast-enhancement in MRI

In MRI, CE was present in 18/20 patients (90.0%); in two patients with newly diagnosed *IDH*-mutant and *IDH*-wildtype anaplastic astrocytoma (patients 4 and 15) no CE could be detected; both patients showed uptake in ¹⁸F-GE-180 PET, but only one of them showed ¹⁸F-FET uptake significantly exceeding the background activity. In patients with CE, VOL_{CE} [median 9.7 ml (range, 0.1–72.5 ml)] was significantly smaller than the PET-derived BTVs, i.e., BTV_{FET} [median 19.3 ml (range, 0.7–150.2 ml), *p* = 0.001] and BTV_{GE-180} [median 32.1 ml (range, 0.4–236.0 ml), *p* = 0.001]. Thus, only a low spatial correlation between CE and the PET-derived BTVs could be detected with a median Sørensen–Dice coefficient of 0.29 (range, 0.01–0.48) compared to BTV_{GE-180} and

Table 4 Spatial correlation of ¹⁸F-GE-180 and ¹⁸F-FET PET derived BTVs [median Sørensen–Dice-coefficient (range)]

	BTV _{GE-180} vs BTV _{FET}
Total	0.55 (0.07–0.85)
<i>IDH</i> -mutant	0.53 (0.07–0.76)
<i>IDH</i> -wildtype	0.59 (0.32–0.85)
Significance	<i>p</i> = 0.206
WHO grade III	0.33 (0.07–0.63)
WHO grade IV	0.62 (0.20–0.85)
Significance	<i>p</i> = 0.065

0.38 (range, 0.01–0.68) compared to BTV_{FET}. See also Table 5.

Correlation to TSPO-polymorphism

In the current cohort, patients with all three types of binding status (including three patients with LAB) were evaluated. Comparing ¹⁸F-GE-180 PET parameters of LAB, MAB, and HAB patients, there were no significant differences in background activity [median background activity: 0.45 (range, 0.37–0.47) vs 0.36 (range, 0.36–0.54) vs 0.40 (range, 0.32–0.49), *p* = 0.649] or tumoral uptake intensity [median TBR_{max}: 6.27 (range, 4.47–8.95) vs 4.58 (range, 3.43–6.81) vs 4.01 (range, 2.33–6.55); *p* = 0.164]; see also supplementary Fig. 1.

Discussion

Recently, PET imaging using ¹⁸F-GE-180, a novel high-affinity TSPO ligand, has shown high tumour-to-background contrast and tracer uptake exceeding the areas of CE in MRI in glioblastoma patients [25]. This is the first study to compare its uptake characteristics to the amino acid tracer ¹⁸F-FET and contrast-enhanced MRI of the brain in patients with HGG.

In the current cohort of newly diagnosed and recurrent HGG patients, all cases (100%) showed elevated uptake in ¹⁸F-GE-180 PET. Interestingly, *IDH*-wildtype gliomas showed higher uptake intensity than those with *IDH*-mutation, which is in line with the current literature linking TSPO expression with more aggressive tumour features and poor prognosis [8]. Conversely, less aggressive tumour parts and low-grade gliomas have been reported to show no or only low TSPO expression [9].

In ¹⁸F-FET PET, all but one patient (95%) showed uptake significantly exceeding the background activity. The single ¹⁸F-FET-negative case was a newly diagnosed anaplastic astrocytoma (*IDH*-wildtype, WHO grade III). Although ¹⁸F-FET negativity is a feature predominantly linked to *IDH*-mutant gliomas/LGG, it has been reported to occur in 5% of HGG cases [7, 28]. Interestingly, the uptake intensity of ¹⁸F-FET did not differ in relation to the *IDH*-mutational status at all, a direct contrast to ¹⁸F-GE-180 PET.

When directly comparing the uptake intensity of both tracers, HGG seem to have higher uptake of ¹⁸F-GE-180 compared to ¹⁸F-FET (without reaching the level of significance).

Table 5 Spatial correlation of ¹⁸F-GE-180 and ¹⁸F-FET PET derived BTVs and CE in MRT [median Sørensen–Dice coefficient (range)]

	VOL _{CE} vs BTV _{FET}	VOL _{CE} vs BTV _{GE-180}
Sørensen–Dice coefficient	0.38 (0.01–0.68)	0.29 (0.01–0.48)

However, in the subgroups, *IDH*-wildtype gliomas showed significantly higher uptake intensity in ^{18}F -GE-180 compared to ^{18}F -FET PET, while the uptake intensities of both tracers seem to be comparable in *IDH*-mutant gliomas. Notably, when looking at the individual scans, only 5/20 patients (25.0%) showed higher TBR_{max} in ^{18}F -FET PET compared to ^{18}F -GE-180 PET; interestingly, all five cases were *IDH*-mutant gliomas. By analogy, higher uptake in ^{18}F -GE-180 PET compared to ^{18}F -FET PET was observed in WHO grade IV gliomas as well, but not in WHO grade III gliomas; this might be explained by the high inter-correlation of *IDH*-mutational status and WHO grades.

Moreover, the comparison of relative TBR_{max} values showed a significantly higher relative TBR_{max} in *IDH*-wildtype gliomas (i.e., median 1.55-fold higher TBR_{max} in ^{18}F -GE-180 PET, up to 2.05-fold higher TBR_{max}) compared to *IDH*-mutant gliomas (i.e., median 1.05-fold higher TBR_{max} in ^{18}F -GE-180 PET), with ratios < 1 in *IDH*-mutant gliomas only.

Comparing plain SUV values without background reference, similar results could be obtained to those using TBR_{max} values with regard to the *IDH*-mutational status and WHO grades using both tracers, although plain SUV values are distinctly higher in ^{18}F -FET PET compared to ^{18}F -GE-180 PET overall and in subgroup analyses. Nonetheless, assessment of TBR values is common sense in neurooncological PET imaging, as recently emphasized in the joint RANO/EANO/EANM/SNMMI procedure guidelines [39].

Our findings lead to the assumption that ^{18}F -GE-180 PET might be particularly valuable for the depiction of tumour features attributed to poor prognosis (i.e., *IDH*-wildtype), while ^{18}F -FET, which has also proven itself capable in the evaluation of less aggressive tumours such as LGG [35], might show favorable imaging characteristics compared to ^{18}F -GE-180 for the depiction of tumours (or tumour parts) with less aggressive biological behaviour. In particular, ^{18}F -FET shows a very high uptake intensity in gliomas with *IDH*-mutation and additional 1p/19q-codeletion (i.e., oligodendroglial tumours) [40], which knowingly present with best prognosis among the distinct molecular genetic subtypes [27]; in the current study, four cases of anaplastic oligodendroglioma were included; in three of the four cases, a distinctly higher uptake in PET with ^{18}F -FET compared to ^{18}F -GE-180 was detected.

In the analysis of dynamic ^{18}F -FET PET, TTP_{min} is considered an important prognostic factor in gliomas [28, 36, 41]. In the current set of patients, TTP_{min} in dynamic ^{18}F -FET PET did not correlate with the uptake intensity or BTv in ^{18}F -GE-180 PET, which is an interesting finding, as one might have expected an association between both prognostically relevant factors TTP_{min} and TSPO expression.

Jensen et al. spatially correlated amino acid uptake and TSPO expression using ^{123}I -CLINDE SPECT and ^{18}F -FET

PET in a first small set of three glioblastoma patients, and described a diverging overlap of these modalities [26]. These preliminary results are in line with our findings: although the absolute volumes derived in both PET modalities were statistically indifferent, there was only a moderate spatial correlation of these volumes, with a spatial overlap of around 50%, which is a surprisingly low percentage. When subdivided into WHO grades, there was a higher, but still only moderate overlap of around 60% in WHO grade IV, but an even lower overlap of around 30% in WHO grade III gliomas (see Table 4). This indicates that both PET modalities do substantially differ regarding their imaging information, in particular taking into account the underlying *IDH*-mutational status and WHO grades. Keeping in mind the low expression of LGG and less aggressive tumour parts, combined imaging might therefore non-invasively enable characterization of tumour heterogeneity. Here, combined imaging might, for example, permit improved tumour grading, identification of the most aggressive areas within gliomas and the underlying molecular genetic features, as dynamic ^{18}F -FET PET so far seems to be associated with the individual *IDH*-mutation status, irrespective of an additional 1p/19q-codeletion [42, 43].

In clinical routine, MRI represents the diagnostic gold standard, with CE representing the target of local therapies. Hence, we correlated the PET-based BTVs with the volumes of CE in MRI. VOL_{CE} was significantly smaller compared to the BTVs in both PET modalities. Consequently, a low spatial correlation of VOL_{CE} and the respective BTVs with a mean spatial overlap of around 30% only could be detected. These values are even lower than in the first study evaluating ^{18}F -GE-180 PET in *IDH*-wildtype glioblastomas [25], possibly due to the currently more heterogeneous cohort including different molecular genetic features. As both PET-derived BTVs have shown a mean spatial overlap of around 50% themselves, only, this indicates a high diagnostic potential of dual PET imaging targeting amino acid uptake and TSPO expression in HGG, in addition to the clinical gold standard MRI of the brain. Patient examples are displayed in Figs. 1 and 2.

As seen in a previous ^{18}F -GE-180 PET study in patients with relapsing-remitting multiple sclerosis [24], the current 20 scans did not provide a major association of ^{18}F -GE-180 binding characteristics with the individual binding status, as all patients with LAB status showed extraordinary high uptake and TBR_{max} even beyond CE in MRI, although, of course, no statistically valid conclusion can be drawn with only three included LAB. Using kinetic modeling, no major dependencies between HAB and MAB patients were observed in healthy subjects [22]. Moreover, using SUVR images, even patients classified as LAB suffering multiple sclerosis showed high focal uptake [24], indicating that LAB patients should not be excluded from studies in general. However, additional studies evaluating different quantification approaches are

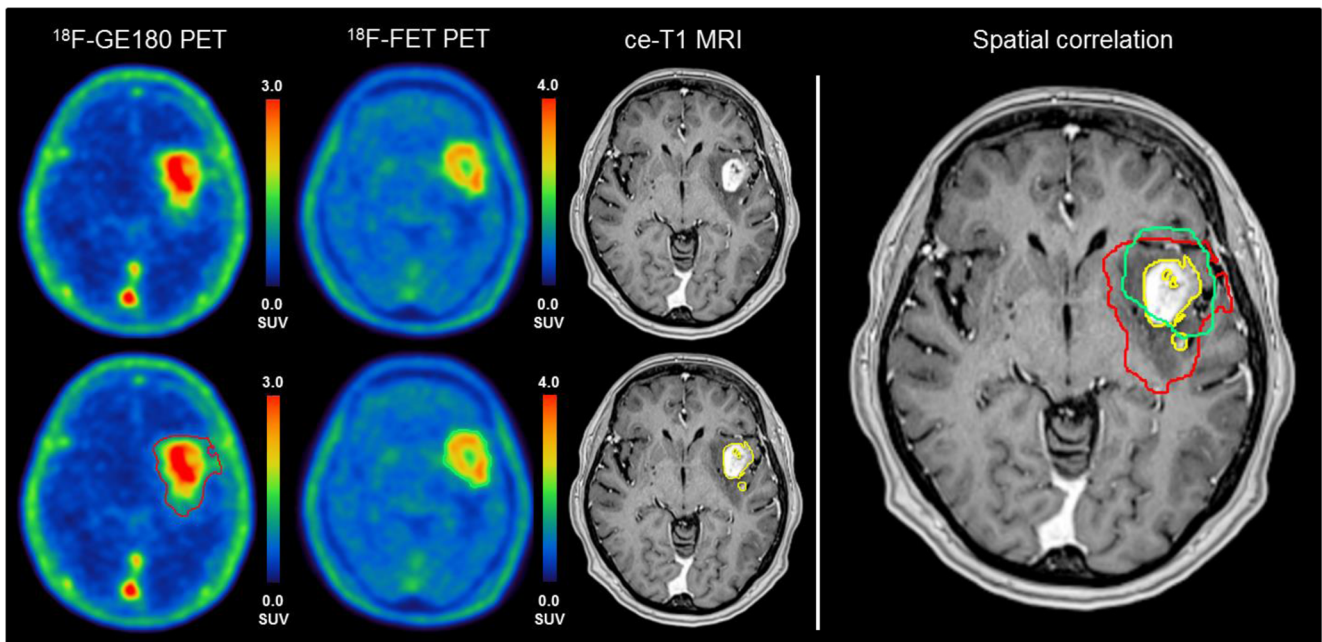


Fig. 1 In a case of newly diagnosed, *IDH*-wildtype glioblastoma (patient 11) there is a moderate spatial correlation of BTV_{GE-180} (red line) and BTV_{FET} (green line) and just a low spatial correlation of VOL_{CE} (yellow line) with the PET-based BTVs

warranted in patients with LAB status. Moreover, there is no data regarding non-specific binding and potential off-target binding in humans so far. Although preclinical studies using microglial staining, evaluation of TSPO-expression with polymerase-chain-reaction, and blocking in rodents do indicate specific binding and do not speak

for off-target binding [44–46], further studies in humans have to address these issues and correlate them with the individual binding status.

Interestingly, two patients did not show CE — as surrogate for BBB breakdown — in MRI, but showed distinct uptake in ^{18}F -GE-180 PET, which also indicates that binding of ^{18}F -

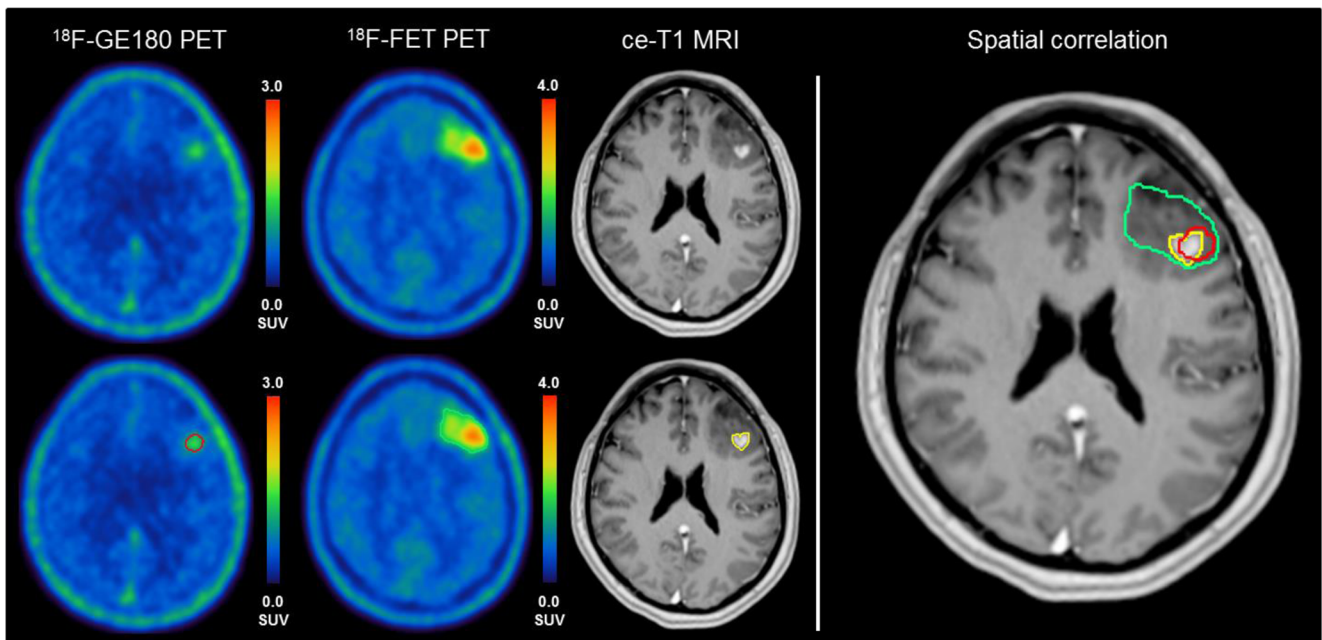


Fig. 2 In a case of newly diagnosed anaplastic oligodendroglioma (*IDH*-mutant, 1p/19q-codeletion, patient 9) BTV_{FET} (green line) shows a poor spatial correlation with BTV_{GE180} (red line) and VOL_{CE} (yellow line),

whereas there is a higher, but still just moderate spatial correlation of BTV_{GE-180} and VOL_{CE}

GE-180 is not caused by a mere breakdown of the BBB, as also seen in non-CE lesions in patients with multiple sclerosis [24]. Nonetheless, a certain “micro leakage” of the BBB facilitating the crossing of ^{18}F -GE-180 in the brain, but not enabling the crossing of the larger molecules of gadolinium, has to be considered in this context, as ^{18}F -GE-180 does not seem to easily penetrate the healthy brain as represented by a relatively low background activity. As discussed previously [23], the high binding to plasma proteins needs to be considered as a factor influencing the penetration of ^{18}F -GE-180 in the healthy brain tissue. Also, this high plasma binding might contribute to the rather high signal in blood vessels. In sum, in humans no data is available with regard to the exact contribution of the BBB integrity to ^{18}F -GE-180 uptake in gliomas. Therefore, further studies in humans have to address this issue of the exact contribution of plasma binding and BBB integrity with regard to the particular ^{18}F -GE-180 uptake.

Nonetheless, for translation of TSPO PET in the clinical setting, further studies are needed elucidating the relation of TSPO expression of tumour-associated neuroinflammatory and neoplastic cells. Although studies have reported that TSPO expression in gliomas is predominantly related to neoplastic cells [9, 12], further studies using step-wise stereotactic biopsies in spatial correlation to the PET information are warranted. As part of this process, specific thresholds for TSPO uptake quantification in ^{18}F -GE-180 PET have to be evaluated, as the currently used threshold of $\text{SUV}_{\text{BG}} \times 1.8$ represents an arbitrary cut-off for approximate estimation and comparisons of BTVs, which, however, allows an objective, reader-independent, and uniform estimation of the tumour volume and, consequently, a spatial comparison of the patterns of distribution with further modalities. As approaches using tentative thresholds allow only an approximate estimation of spatial overlaps in comparison to CE and amino acid uptake, with further dependencies of the chose cut-off value, a histologically verified threshold, as available for ^{18}F -FET PET [47], is urgently needed for further comprehensive studies focusing on ^{18}F -GE-180 PET in patients with brain tumours.

Conclusion

PET with ^{18}F -GE-180 and ^{18}F -FET provides differing imaging information in HGG dependent on the *IDH*-mutational status, with a diverging spatial overlap and a high exceedance of contrast-enhancing tumour parts in MRI. Combined imaging might reveal new insights with regard to non-invasive characterization of tumour heterogeneity, and might influence the patients' management in terms of treatment planning and response assessment.

Acknowledgements We thank Dr. V. Milenkovic for the support regarding polymorphism genotyping. Additionally, we thank Joanne Stevens and GE-Healthcare for the support regarding tracer production.

Compliance with ethical standards

Conflict of interest All authors declare that they have no relationships or interests that could have direct or potential influence or impart bias on the work.

Ethical approval The study was authorized by the local ethics committee (IRB 17–769) in accordance with the ICH Guideline for Good Clinical Practice (GCP) and the Declaration of Helsinki.

Informed consent All patients gave written consent to participate in the study.

References

1. Wen PY, Macdonald DR, Reardon DA, Cloughesy TF, Sorensen AG, Galanis E, et al. Updated response assessment criteria for high-grade gliomas: Response Assessment in Neuro-Oncology Working Group. *J Clin Oncol*. 2010;28:1963–72.
2. Watanabe M, Tanaka R, Takeda N. Magnetic resonance imaging and histopathology of cerebral gliomas. *Neuroradiology*. 1992;34:463–9.
3. Suchorska B, Jansen NL, Linn J, Kretschmar H, Janssen H, Eigenbrod S, et al. Biological tumor volume in ^{18}F FET-PET before radiochemotherapy correlates with survival in GBM. *Neurology*. 2015;84:710–9.
4. Galldiks N, Langen KJ, Pope WB. From the clinician's point of view — what is the status quo of positron emission tomography in patients with brain tumors? *Neuro Oncol*. 2015;7(11):1434–44.
5. Albert NL, Weller M, Suchorska B, Galldiks N, Soffietti R, Kim MM, et al. Response Assessment in Neuro-Oncology Working Group and European Association for Neuro-Oncology recommendations for the clinical use of PET imaging in gliomas. *Neuro Oncol*. 2016;18:1199–208.
6. Habemeier A, Graf J, Sandhöfer BF, Boissel J-P, Roesch F, Closs EI. System 1 amino acid transporter LAT1 accumulates O-(2-fluoroethyl)-l-tyrosine (FET). *Amino Acids*. 2015;47:335–44. <https://doi.org/10.1007/s00726-014-1863-3>.
7. Unterrainer M, Schweisthal F, Suchorska B, Wenter V, Schmid-Tannwald C, Fendler WP, et al. Serial ^{18}F -FET PET imaging of primarily ^{18}F -FET-negative glioma: does it make sense? *J Nucl Med*. 2016;57:1177–82.
8. Vlodavsky E, Soustiel JF. Immunohistochemical expression of peripheral benzodiazepine receptors in human astrocytomas and its correlation with grade of malignancy, proliferation, apoptosis and survival. *J Neurooncol*. 2007;81:1–7.
9. Su Z, Roncaroli F, Durrenberger PF, Coope DJ, Karabatsou K, Hinz R, et al. The 18-kDa mitochondrial translocator protein in human gliomas: an ^{11}C -(R)PK11195 PET imaging and neuropathology study. *J Nucl Med*. 2015;56:512–7.
10. Awde AR, Boisgard R, Theze B, Dubois A, Zheng J, Dolle F, et al. The translocator protein radioligand ^{18}F -DPA-714 monitors antitumor effect of erufosine in a rat 9L intracranial glioma model. *J Nucl Med*. 2013;54:2125–31.
11. Buck JR, McKinley ET, Fu A, Abel TW, Thompson RC, Chambless L, et al. Preclinical TSPO ligand PET to visualize human glioma xenotransplants: a preliminary study. *PLoS One*. 2015;10:e0141659.

12. Winkeler A, Boisgard R, Awde AR, Dubois A, Theze B, Zheng J, et al. The translocator protein ligand [(1)(8)F]DPA-714 images glioma and activated microglia in vivo. *Eur J Nucl Med Mol Imaging*. 2012;39:811–23.
13. Tang D, Nickels ML, Tantawy MN, Buck JR, Manning HC. Preclinical imaging evaluation of novel TSPO-PET ligand 2-(5,7-Diethyl-2-(4-(2-[(18)F]fluoroethoxy)phenyl)pyrazolo[1,5-a]pyrimidin-3-yl)-N,N-diethylacetamide ([(18)F]VUIIS1008) in glioma. *Molec Imaging Biol*. 2014;16:813–20.
14. Takaya S, Hashikawa K, Turkheimer FE, Mottram N, Deprez M, Ishizu K, et al. The lack of expression of the peripheral benzodiazepine receptor characterises microglial response in anaplastic astrocytomas. *J Neurooncol*. 2007;85:95–103.
15. Junck L, Olson JM, Ciliax BJ, Koeppe RA, Watkins GL, Jewett DM, et al. PET imaging of human gliomas with ligands for the peripheral benzodiazepine binding site. *Ann Neurol*. 1989;26:752–8. <https://doi.org/10.1002/ana.410260611>.
16. Pappata S, Cornu P, Samson Y, Prenant C, Benavides J, Scatton B, et al. PET study of carbon-11-PK 11195 binding to peripheral type benzodiazepine sites in glioblastoma: a case report. *J Nucl Med*. 1991;32:1608–10.
17. Wadsworth H, Jones PA, Chau WF, Durrant C, Fouladi N, Passmore J, et al. [(1)(8)F]GE-180: a novel fluorine-18 labelled PET tracer for imaging translocator protein 18 kDa (TSPO). *Bioorg Med Chem Lett*. 2012;22:1308–13.
18. Boutin H, Murray K, Pradillo J, Maroy R, Smigova A, Gerhard A, et al. 18F-GE-180: a novel TSPO radiotracer compared to 11C-R-PK11195 in a preclinical model of stroke. *Eur J Nucl Med Mol Imaging*. 2015;42:503–11.
19. Dickens AM, Vainio S, Marjamaki P, Johansson J, Lehtiniemi P, Rokka J, et al. Detection of microglial activation in an acute model of neuroinflammation using PET and radiotracers 11C-(R)-PK11195 and 18F-GE-180. *J Nucl Med*. 2014;55:466–72.
20. Sridharan S, Lepelletier F-X, Trigg W, Banister S, Reekie T, Kassiou M, et al. Comparative evaluation of three TSPO PET radiotracers in a LPS-induced model of mild neuroinflammation in rats. *Mol Imaging Biol*. 2017;19:77–89.
21. Fan Z, Calsolaro V, Atkinson RA, Femminella GD, Waldman A, Buckley C, et al. Flutriciclamide (18F-GE180) PET: first in human PET study of novel 3rd generation in vivo marker of human translocator protein. *J Nucl Med*. 2016;57(11):1753–1759.
22. Feeney C, Scott G, Raffel J, Roberts S, Coello C, Jolly A, et al. Kinetic analysis of the translocator protein positron emission tomography ligand [18F]GE-180 in the human brain. *Eur J Nucl Med Mol Imaging*. 2016;43:2201–10.
23. Vomacka L, Albert NL, Lindner S, Unterrainer M, Mahler C, Brendel M, et al. TSPO imaging using the novel PET ligand [18F]GE-180: quantification approaches in patients with multiple sclerosis. *EJNMMI Res*. 2017;7:89.
24. Unterrainer M, Mahler C, Vomacka L, Lindner S, Havla J, Brendel M, et al. TSPO PET with [18F]GE-180 sensitively detects focal neuro-inflammation in patients with relapsing-remitting multiple sclerosis. *Eur J Nucl Med Mol Imaging*. 2018;45:1423–31.
25. Albert NL, Unterrainer M, Fleischmann D, Lindner S, Vettermann F, Brunegrab A, et al. TSPO PET for glioma imaging using the novel ligand 18F-GE-180: first results in patients with glioblastoma. *Eur J Nucl Med Mol Imaging*. 2017;44(13):2230–2238.
26. Jensen P, Feng L, Law I, Svarer C, Knudsen GM, Mikkelsen JD, et al. TSPO imaging in glioblastoma multiforme: a direct comparison between 123I-CLINDE SPECT, 18F-FET PET, and gadolinium-enhanced MR imaging. *J Nucl Med*. 2015;56:1386–90.
27. Louis DN, Perry A, Reifenberger G, Von Deimling A, Figarella-Branger D, Cavenee WK, et al. The 2016 World Health Organization classification of tumors of the central nervous system: a summary. *Acta Neuropathol*. 2016;131:803–20.
28. Suchorska B, Giese A, Biczok A, Unterrainer M, Weller M, Drexler M, et al. Identification of time-to-peak on dynamic 18F-FET-PET as a prognostic marker specifically in IDH1/2 mutant diffuse astrocytoma. *Neurooncol*. 2017;20(2):279–288.
29. Eigenbrod S, Trabold R, Brucker D, Erös C, Egensperger R, La Fougere C, et al. Molecular stereotactic biopsy technique improves diagnostic accuracy and enables personalized treatment strategies in glioma patients. *Acta Neurochir*. 2014;156:1427–40.
30. Owen DR, Gunn RN, Rabiner EA, Bennacef I, Fujita M, Kreisl WC, et al. Mixed-affinity binding in humans with 18-kDa translocator protein ligands. *Journal of nuclear medicine : official publication. Soc Nucl Med*. 2011;52:24–32.
31. Owen DR, Yeo AJ, Gunn RN, Song K, Wadsworth G, Lewis A, et al. An 18-kDa translocator protein (TSPO) polymorphism explains differences in binding affinity of the PET radioligand PBR28. *J Cereb Blood Flow Metab*. 2012;32:1–5.
32. Guo Q, Owen DR, Rabiner EA, Turkheimer FE, Gunn RN. Identifying improved TSPO PET imaging probes through biomathematics: the impact of multiple TSPO binding sites in vivo. *NeuroImage*. 2012;60:902–10.
33. Wickström T, Clarke A, Gausemel I, Horn E, Jørgensen K, Khan I, et al. The development of an automated and GMP compliant FASTlab™ synthesis of [18F] GE-180; a radiotracer for imaging translocator protein (TSPO). *J Label Compd Radiopharm*. 2014;57:42–8.
34. Unterrainer M, Vettermann F, Brendel M, Holzgreve A, Lifschitz M, Zähringer M, et al. Towards standardization of 18 F-FET PET imaging: do we need a consistent method of background activity assessment? *EJNMMI Res*. 2017;7:48.
35. Jansen NL, Graute V, Armbruster L, Suchorska B, Lutz J, Eigenbrod S, et al. MRI-suspected low-grade glioma: is there a need to perform dynamic FET PET? *Eur J Nucl Med Mol Imaging*. 2012;39:1021–9.
36. Jansen NL, Suchorska B, Wenter V, Schmid-Tannwald C, Todica A, Eigenbrod S, et al. Prognostic significance of dynamic 18F-FET PET in newly diagnosed astrocytic high-grade glioma. *J Nucl Med*. 2015;56:9–15.
37. Dice LR. Measures of the amount of ecologic association between species. *Ecology*. 1945;26:297–302.
38. Sørensen T. A method of establishing groups of equal amplitude in plant sociology based on similarity of species and its application to analyses of the vegetation on Danish commons. *Biol Skr*. 1948;5:1–34.
39. Law I, Albert NL, Arbizu J, Boellaard R, Drzezga A, Galldiks N, et al. A joint RANO/EANO/EANM Practice Guideline/SNMMI Procedure Standard for Imaging of Gliomas using PET with Radiolabeled Amino Acids and [18F]FDG: Version 1.0. SNMMI Publications. 2018.
40. Jansen NL, Schwartz C, Graute V, Eigenbrod S, Lutz J, Egensperger R, et al. Prediction of oligodendroglial histology and LOH 1p/19q using dynamic [18F] FET-PET imaging in intracranial WHO grade II and III gliomas. *Neurooncol*. 2012;14:1473–80.
41. Jansen NL, Suchorska B, Wenter V, Eigenbrod S, Schmid-Tannwald C, Zwerger A, et al. Dynamic 18F-FET PET in newly diagnosed astrocytic low-grade glioma identifies high-risk patients. *J Nucl Med*. 2014;55:198–203.
42. Verger A, Stoffels G, Bauer EK, Lohmann P, Blau T, Fink GR, et al. Static and dynamic 18F-FET PET for the characterization of gliomas defined by IDH and 1p/19q status. *Eur J Nucl Med Mol Imaging*. 2018;45(3):443–451.
43. Unterrainer M, Winkelmann I, Suchorska B, Giese A, Wenter V, Kreth FW, et al. Biological tumour volumes of gliomas in early and standard 20–40 min 18F-FET PET images differ according to IDH mutation status. *Eur J Nucl Med Mol Imaging*. 2018;45:1242–9. <https://doi.org/10.1007/s00259-018-3969-4>.

44. Brendel M, Focke C, Blume T, Peters F, Deussing M, Probst F, et al. Time courses of cortical glucose metabolism and microglial activity across the life span of wild-type mice: a PET study. *J Nucl Med*. 2017;58:1984–90.
45. Deussing M, Blume T, Vomacka L, Mahler C, Focke C, Todica A, et al. Coupling between physiological TSPO expression in brain and myocardium allows stabilization of late-phase cerebral [18F] GE180 PET quantification. *NeuroImage*. 2018;165:83–91.
46. Deussing M, Blume T, Vomacka L, Mahler C, Focke C, Todica A, et al. Data on specificity of [18F] GE180 uptake for TSPO expression in rodent brain and myocardium. *Data Brief*. 2018;19:331–6.
47. Pauleit D, Floeth F, Hamacher K, Riemenschneider MJ, Reifenberger G, Muller HW, et al. O-(2-[18F]fluoroethyl)-L-tyrosine PET combined with MRI improves the diagnostic assessment of cerebral gliomas. *Brain*. 2005;128:678–87.